Article

Boolean Control of Aptamer Binding States

Dmitry M. Kolpashchikov, and Milan N. Stojanovic

J. Am. Chem. Soc., **2005**, 127 (32), 11348-11351• DOI: 10.1021/ja051362f • Publication Date (Web): 20 July 2005

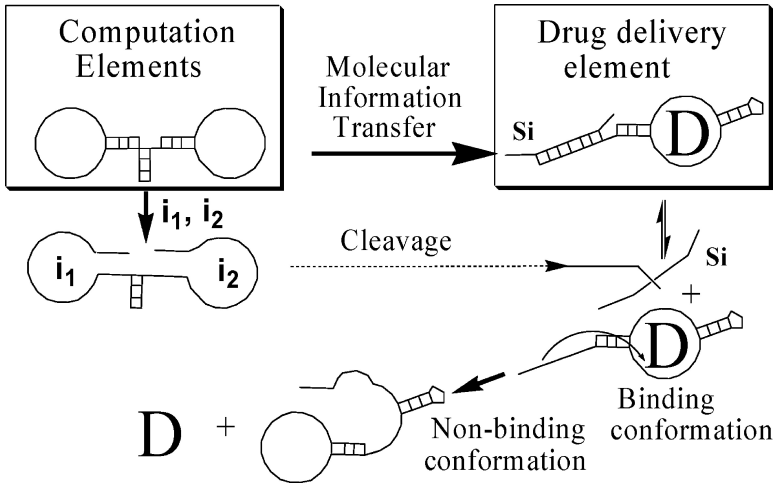

More About This Article

Additional resources and features associated with this article are available within the HTML version:

- Supporting Information
- Links to the 14 articles that cite this article, as of the time of this article download
- Access to high resolution figures
- Links to articles and content related to this article
- Copyright permission to reproduce figures and/or text from this article

View the Full Text HTML

J|A|C|S
ARTICLES
Published on Web 07/20/2005

Boolean Control of Aptamer Binding States

Dmitry M. Kolpashchikov and Milan N. Stojanovic*

Contribution from the Division of Experimental Therapeutics, Department of Medicine, Columbia University, Box 84, 630W 168th Street, New York, New York 10032

Received March 3, 2005; E-mail: mns18@columbia.edu

Abstract: Molecules that perform Boolean calculations can analyze a series of inputs and make a decision to produce or not to produce an output, based on the presence or absence of inputs and a particular formula they encode. We now report that molecular computation performed by deoxyribozyme-based logic gates can be used to control the functional state of aptamers, switching them on or off based on the outcome of such computation.

Introduction

We recently reported a solution-phase molecular-scale computation media with elementary "Lego-like" unit deoxyribozyme-based logic gate.[1] In our approach, we combined the concept of molecular logic gates[2] with DNA computation[3−6] and allowed for the "bottom-up" building of computational complexity in solution, as demonstrated by the synthesis of molecular automata[7] and engineered molecular circuits.[8] Our long-term goal is to use these computational elements to control various downstream events, in a way that is similar to electronic computers controlling macroscopic machines.[3]

In all our previous cases, molecular-scale computation has been used to control intrinsic catalytic antisense activity of deoxyribozymes, which was visualized through fluorogenic cleavage of labeled substrate. In amazing reaction cascades[9] behaving as molecular automata, Shapiro's group was able to release the final product oligonucleotides, with a potential for stoichiometric antisense activity. We now demonstrate for the first time that an output of molecular computation can be connected to a downstream event other than cleavage or formation of oligonucleotides. Specifically, we trigger the release of a small molecule (malachite green) and control enzymatic activity (Taq DNA polymerase) via molecular computation. These proof-of-concept results bring us closer to the construction of autonomous therapeutic devices with molecular-scale computation elements analyzing multiple disease markers and deciding to kill or not to kill a cell because we have achieved a molecular information transfer resulting in the translation of antisense outputs into other molecular events (Figure 1).

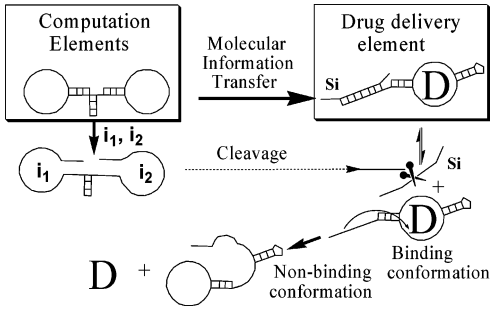

Figure 1. A molecular network consisting of a computation element analyzing oligonucleotide inputs (in this case, an $\mathbf{i_1ANDi_2}$ gate) and signaling to a drug delivery element (a structure switching aptamer) to release a drug (**D**). The molecular information transfer occurs through the active gate (complexed with inputs i_1 and i_2) cleaving substrate ($\mathbf{S_i}$) that is keeping the aptamer in a binding conformation. The removal of a substrate by an active gate causes the structure to switch to the nonbinding conformation, due to a shift in equilibrium, and the drug is released.

Results and Discussion

To integrate new output-producing elements into molecular circuits, we constructed two-state aptamers, similar to the state-switching aptamers used before in molecular machines, sensors, and a hybridization chain reaction,[10] and active only in the presence of an input oligonucleotide $\mathbf{S_i}$ with a single chimeric rA position (Figure 2). Such a two-state aptamer could receive information from an upstream molecular logic gate which either cleaves $\mathbf{S_i}$, or not, based on solution inputs and its truth table. The information in this cascade is transferred from an upstream logic gate to a downstream aptameric unit through a common component, which serves as a substrate for the former, and as an allosteric effector for the latter unit.

For the initial test of our ability to couple conformational changes in engineered aptamers to Boolean calculations by deoxyribozymes, we chose an aptamer that binds malachite

(1) Stojanovic, M. N.; Mitchell, T. E.; Stefanovic, D. *J. Am. Chem. Soc.* **2002**, *124*, 3555.
(2) De Silva, A. P.; McClenaghan, N. D. *Chemistry* **2004**, *10*, 574 and references therein.
(3) Braich, R. S.; Chelyapov, N.; Johnson, C.; Rothemund, P. W. K.; Adleman, L. *Science* **2002**, *296*, 499.
(4) Winfree, E.; Liu, F. R.; Wenzler, L. A.; Seeman, N. C. *Nature* **1998**, *394*, 539.
(5) Benenson, Y.; Paz-Elizur, T.; Adar, R.; Keinan, E.; Livneh, Z.; Shapiro, E. *Nature* **2001**, *414*, 430.
(6) Wang, H.; Hall, J. G.; Liu, Q.; Smith, L. M. *Nat. Biotechnol*. **2001**, *19*, 1053.
(7) Stojanovic, M. N.; Stefanovic, D. *Nat. Biotechnol*. **2003**, *21*, 1069.
(8) Stojanovic, M. N.; Stefanovic, D. J. *J. Am. Chem. Soc.* **2003**, *125*, 6673.
(9) Benenson, Y.; Gil, B.; Ben-Dor, U.; Adar, R.; Shapiro, E. *Nature* **2004**, *429*, 423.
(10) (a) Dittmer, W. U.; Reuter, A.; Simmel, F. C. *Angew. Chem., Int. Ed.* **2004**, *43*, 3550. (b) Dirks, R. M.; Pierce, N. A. *Proc. Natl. Acad. Sci. U.S.A.* **2004**, *101* 15275. (c) Nutiu, R.; Li, Y. *J. Am. Chem. Soc.* **2003**, *125*, 4771.

10.1021/ja051362f CCC: $30.25

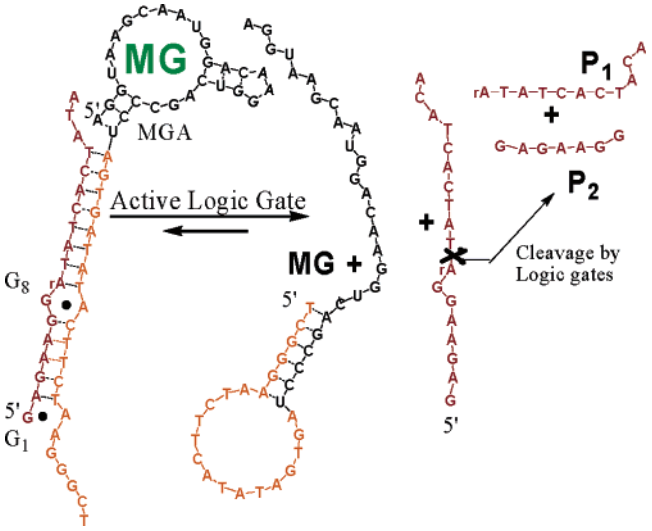

Figure 2. The malachite green aptamer exists in two conformations (binding and fluorescent, and nonbinding or dark; that is, complexed with $\mathbf{S_i}$ or not complexed with $\mathbf{S_i}$, respectively), which are switched based on the result of Boolean calculations from the upstream **AND** gate.

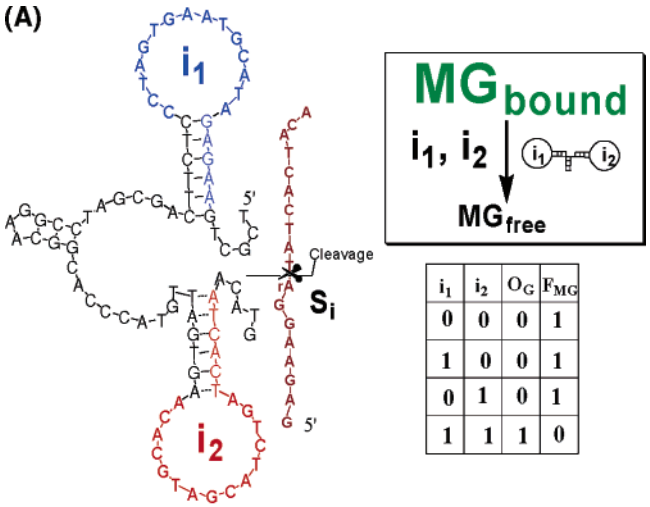

i_1	i_2	O_G	F_{MG}
0	0	0	1
1	0	0	1
0	1	0	1
1	1	1	0

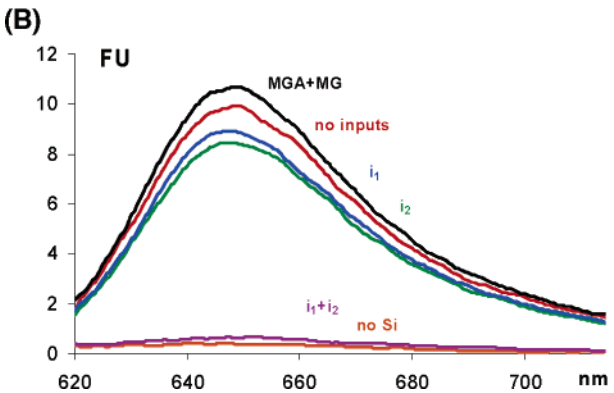

Figure 3. (A) Structure of $\mathbf{i_1ANDi_2}$ gate, which was incorporated in the cascade shown in Figure 2. Gate triggers the release of malachite green from its aptamer. The truth table contains the gate state ($\mathbf{O}_G$) and the fluorescence of malachite green as outputs ($\mathbf{F}_{MG}$). (B) The emitting spectra after 6 h of incubation (λ_{ex} = 600 nm) (all samples have MGA and MG). Black spectra: positive control, no gate and no inputs. Red spectra: both inputs absent. Blue spectra: only i_1. Green spectra: only i_2. Maroon spectra: both inputs. Orange spectra: no substrate $\mathbf{S_i}$.

green (**MGA**, $K_d \sim 120$ nM).[11] Malachite green (**MG**) is almost nonfluorescent while free in solution, but becomes strongly

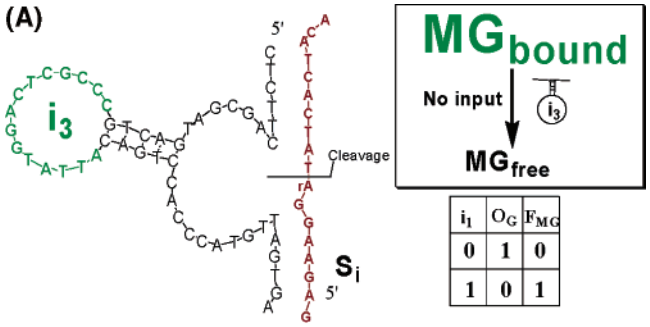

i_1	O_G	F_{MG}
0	1	0
1	0	1

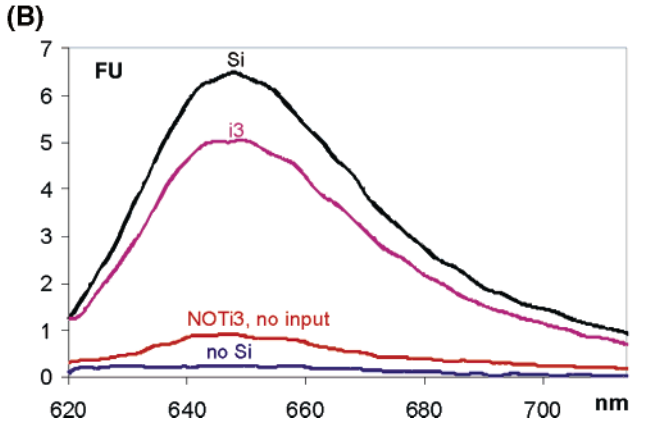

Figure 4. (A) Structure of $\mathbf{NOTi_3}$ gate, which was incorporated in a cascade similar to the one shown in Figure 2. Gate triggers the release of malachite green from its aptamer in the absence of oligonucleotide i_3. The truth table contains the gate state ($\mathbf{O}_G$) and the fluorescence of malachite green as outputs ($\mathbf{F}_{MG}$). (B) The fluorescence intensity after 20 h of incubation (λ_{ex} = 600 nm) (all samples have MGA and MG). Blue spectra: no $\mathbf{S_i}$. Black spectra: positive control, no gate and no inputs. Orange spectra: $\mathbf{NOTi_3}$, no input. Maroon spectra: in the presence of oligonucleotide input $\mathbf{i_3}$.

fluorescent when complexed with its aptamer,[12] and we previously used this characteristic to construct sensors for small molecules and short oligonucleotides.[13] This characteristic provides us with a straightforward way of detecting the state of the aptamer, which can be binding (**1**) or nonbinding (**0**).

A two-state switch version of **MGA** consists of a malachite green binding module and an extension region; the extension can bind either $\mathbf{S_i}$ or the malachite green binding module, but not both (Figure 2). Thus, in the presence of $\mathbf{S_i}$, the aptamer would become active and bind **MG**, while upon the removal of $\mathbf{S_i}$, through the catalytic reaction of a deoxyribozyme gate, the aptamer module should become inactive and release the dye. The molecular information transfer between gates and two-state aptamers occurs through the law of mass action because current gates cannot cleave $\mathbf{S_i}$ in complexes, but will remove the free $\mathbf{S_i}$ present in solution. Two mismatches (G1 and G8) between $\mathbf{S_i}$ and the allosteric aptamer were deliberately introduced with two intended functions: (1) they necessitate an excess of $\mathbf{S_i}$ in solution to shift equilibrium toward complex formation; and (2) they facilitate the release of $\mathbf{S_i}$ and conformational switching, leading to the discharge of **MG**. We demonstrated (Supporting Information) that a 1 μM concentration of the aptamer will start releasing the **MG** when the concentration of $\mathbf{S_i}$ drops below 2 μM.

(11) Grate, D.; Wilson, C. *Proc. Natl. Acad. Sci. U.S.A.* **1999**, *96*, 6131.
(12) Babendure, J. R.; Adams, S. R.; Tsien, R. Y. *J. Am. Chem. Soc.* **2003**, *125*, 14716.
(13) (a) Stojanovic, M. N.; Kolpashchikov, D. M. *J. Am. Chem. Soc.* **2004**, *126*, 9266. (b) Stojanovic, M. N. *J. Serb. Chem. Soc.* **2004**, *69*, 81.

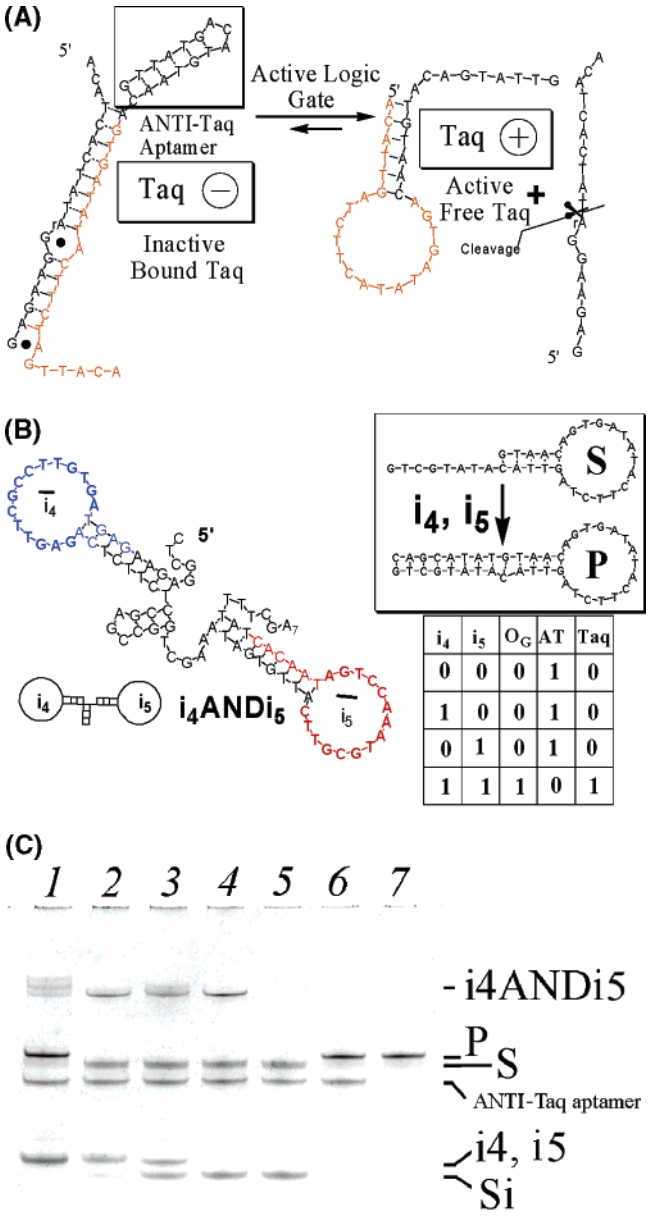

i_4	i_5	O_G	AT	Taq
0	0	0	1	0
1	0	0	1	0
0	1	0	1	0
1	1	1	0	1

Figure 5. (A) The cascade consisting of $\mathbf{i_4ANDi_5}$ gate activating an anti-Taq DNA polymerase aptamer allosterically regulated by its substrate $\mathbf{S_i}$ (in truth table: $\mathbf{O_G}$ gate activity as output, **AT** anti-Taq aptamer as an output, **Taq** polymerase activity as an output). (B) Structures of $\mathbf{i_4ANDi_5}$ gate, substrate **S** and product **P**, which were incorporated in the cascade shown in (A); the truth table contains the gate ($\mathbf{O_G}$), aptamer (**AT**), and enzyme (**Taq**) activity states. (C) Elongation of substrate **S** to product **P** by Taq DNA polymerase. Lane 1: full reaction mixture contained 0.5 μM **S**, $\mathbf{S_i}$, $\mathbf{i_3}$, $\mathbf{i_4}$, 0.2 μM anti-Taq aptamer, and 0.1 μM $\mathbf{i_4ANDi_5}$. Lane 2: in the absence of $\mathbf{i_4}$. Lane 3: in the absence of $\mathbf{i_5}$. Lane 4: both $\mathbf{i_4}$ and $\mathbf{i_5}$ missing. Lane 5: control no $\mathbf{i_4ANDi_5}$ and no inputs. Lane 6: control no $\mathbf{S_i}$, $\mathbf{i_4ANDi_5}$, and both inputs. Lane 7: control with only Taq DNA polymerase substrate **S** added. Note that elongation of $\mathbf{i_4ANDi_5}$ gate in lane 1 was observed, due to DNA polymerase activity and imperfect digital behavior with visible substrate $\mathbf{S_i}$ cleavage, in the presence of only $\mathbf{i_4}$.

In Figure 3, we provide an experimental demonstration of a network with an upstream dual input logic gate ($\mathbf{i_1ANDi_2}$) performing a Boolean calculation and releasing malachite green according to its truth table. The $\mathbf{i_1ANDi_2}$ gate was constructed by the addition of two stem-loops to its substrate recognition regions, as previously described.[1] These stem loops block substrate binding to the deoxyribozyme **E6** core (catalytic nucleic acid with phosphodiesterase activity reported by Breaker and Joyce);[14] however, upon the binding of two input oligonucleotides (i_1 and i_2) to complementary loops, the stems open allowing interactions with the substrate. To minimize the residual and partial stem formation, increase catalytic reaction rates, and, as a result, decrease degradation of RNA components in the mixture, we used 21-mer inputs that overlapped with both loops and parts of the stem (blue and red sequences in Figure 1). A 90% decrease in fluorescence signal (from 8 arbitrary units to 0.6 units) after 6 h with both inputs present (Figure 2B, maroon spectra) indicates that we effectively achieved Boolean control of the release of a small molecule through molecular-scale computation elements, which is also a proof-of-concept experiment for computation-triggered drug release. We also note that the overall circuit behaves as a **NAND** gate with regards to malachite green release and fluorescence (that is, output of **1** from the initial computation in the upstream element produces an output of **0**, that is, no binding and no fluorescence, in the downstream element). A similar result was accomplished with a cascade starting with deoxyribozyme-based **NOT** gate (Figure 4), completing the basic set of logic gates. In the absence of input, oligonucleotide $\mathbf{NOTi_3}$ cleaves $\mathbf{S_i}$ and turns MGA into a nonbinding state (Figure 4B orange line). Addition of $\mathbf{i_3}$ leads to inactivation of $\mathbf{NOTi_3}$ and maintains MGA in a binding conformation (Figure 4B maroon line).

Next, we assembled a Boolean cascade controlling an enzyme, Taq DNA polymerase, through an anti-Taq aptamer, reported by Jayasena and colleagues ($K_d \sim 10$ nM).[15] We attached to the anti-Taq aptamer a region binding to a substrate for upstream logic gates (Figure 5A). If not bound to $\mathbf{S_i}$, this region would bind to an anti-Taq aptamer module, causing the release of the enzyme and activation of the DNA polymerase. We tested our ability to control Taq DNA polymerase activity with an upstream $\mathbf{i_4ANDi_5}$ gate, based on another deoxyribozyme **8**−**17**.[16] In the absence of one or both inputs for the upstream gate, the anti-Taq aptamer remained bound to the protein, leading to the inhibition of its enzymatic activity, as demonstrated by the lack of extension of the oligonucleotide substrate **S** to product **P** (Figure 5c, lanes 2−4). However, in the presence of both inputs, $\mathbf{i_4}$ and $\mathbf{i_5}$, the upstream computation element was activated, cleaving $\mathbf{S_i}$ within 1 h and switching the aptamer to the nonbinding state, leading to the release of enzyme and significant elongation of the substrate to product **P** within 12 h (Figure 5c, lane 1). The delay in the structure switching of aptamer and activation of Taq DNA polymerase was presumably due to the slow off-rate of the tightly bound aptamer and its complex with Taq DNA polymerase keeping it in the active state.

Conclusions

The two examples described above demonstrate that our approach to the Boolean control of aptamers is likely general, and that other aptamers are candidates for integration into molecular circuits. Through the process of in vitro selection and amplification (SELEX) using either natural or unnatural nucleotides, aptamers that are responsive to almost any molecular or ionic species can be isolated, arguing that molecular computation can be connected to almost any other event on a molecular scale.

(14) Breaker, R. R.; Joyce, G. F. *Chem. Biol.* **1995**, *2*, 655.
(15) Dang, C.; Jayasena, S. D. *J. Mol. Biol.* **1996**, *264*, 268−278.
(16) Santoro, S. W.; Joyce, G. F. *Proc. Natl. Acad. Sci. U.S.A.* **1997**, *94*, 4262.

At the beginning of this project, we established molecular computation elements as key components of synthetic molecular devices, envisaged as networks of molecules performing Boolean calculations using multiple phenotype disease markers as inputs, and triggering drug delivery as an output. The current work, although still not suitable for practical in vivo applications, marks a shift in the autonomous computational systems with therapeutic potential from catalytic and stoichiometric antisense outputs to the release of small molecules and control of enzymatic activity.

Materials and Methods

Materials: Oligonucleotides were custom-made and DNA/RNAse free HPLC purified by Integrated DNA Technologies, Inc. (Coralville, IA) and were used as received.

Anti-MG Aptamer: TCG GGC ATC TTC ATA TAG TGA GrCrC rCrGrA rCrUrG rGrArG rCrArG rGrUrA rArCrG rArArU rGrGrC;

Anti-Taq Aptamer: ACA TTG CTC TTC ATA TAG TGA CAA TGT ACA GTA TTG;

S_i: ATA TCA CTA TrAG GAA GAG;

i_1ANDi_2: TCG CTG AAG AGA TAC GTA AGT GAT CCC TCT TCA GCG ATG GCG AAG CCC ACC CAT GTT AGT GAA CAC GTA GCA TCT GAT CAC TAA CAT G;

i_1: GGA TCA CTT ACG TAT CTC TTT;

i_2: TAG TGA TCA GAT GCT ACG TGT;

$NOTi_3$: CTC TTC AGC GAT GAC TGC CCG CTC AGG T AT TAC AGT CCA CCC ATG TTA GTG A;

i_3: TAA TAC CTG AGC GGG;

i_4ANDi_5: CTC GGA GAA GAG TAG TGT TCC GCT TGA GAC TCT TCT CCG AGC CGG TCG AAA TAG TGT TAC TTG CGT AAA CCT GAT AAC ACT ATT TCG AAA AAA A;

i_4: GTC TCA AGC GGA ACA CTA CTC;

i_5: GTG TTA TCA GGT TTA CGC AAGp was protected from elongation by Taq DNA polymerase by 3′ phosphorylation. DNAse/RNAse free water was purchased from ICN (Costa Mesa, CA) and used for all buffers and for stock solutions of oligonucleotides. Malachite green was purchased from Sigma-Aldrich Co. (Milwaukee, WI). Taq DNA polymerase, thermophilic polymerase reaction buffer, 25 mM $MgCl_2$, and 4dNTPs were from Promega, SYBR. Gold was from Molecular Probes.

Instrumental: Fluorescent spectra were taken on a Perkin-Elmer (San Jose, CA) LS-55 luminometer with a Hamamatsu xenon lamp. Experiments were performed at the excitation wavelength of 610 nm and emission scan of 620−700 nm. The spectra were exported to Microsoft Excel files and colored appropriately. The gels were photographed using AlphaImager 3400 (Alpha Innotech).

Control of Malachite Green Binding: Anti-MG aptamer and MG were mixed in binding buffer (50 mM Tris-HCl, pH = 7.4, 50 mM $MgCl_2$, 1 mM NaCl) at the final concentrations of 1 and 0.3 μM, respectively. The concentrations of the individual components were 1.5 μM (**S_i**), 0.2 μM (**i_1ANDi_2** and **$NOTi_3$**), and 0.5 μM (**i1**, **i2**, and **i3**). The reaction mixtures were incubated 6 h for AND gate and 20 h for NOT gate at room temperature in the dark before the fluorescent spectra were taken. Note that fluorescence intensity of the MG−MGA complex decreased approximately 2 times for each 20 h of incubation.

Control of Taq DNA Polymerase Activity: Reaction mixture (20 μL) contained 0.5 μM hairpin DNA substrate **S**, 5 units of Taq DNA polymerase (Promega), 0.2 μM Anti-Taq aptamer, 0.5 μM **S_i**, 0.1 μM **i_3ANDi_4**, 0.5 μM each of the oligonucleotide inputs, if present, reaction buffer (100 mM NaCl, 10 mM Tris-HCl (pH 9.0), 12.5 mM $MgCl_2$, 50 mM KCl, 0.5 mM dNTPs, 0.1% Triton X-100). After 12 h of incubation at 25 °C, 5 μL of each of the reaction mixtures was analyzed by 15% urea PAGE. The gel was stained by SYBR gold and photographed.

Acknowledgment. The funding by the NSF through ITR Medium (EIA-0324845), QuBIC (CCF-0218262), and Biophotonics (BES-0321972) Programs, and NIH (EB-00675) is gratefully acknowledged. M.N.S. is a Searle Scholar.

Supporting Information Available: Graph showing the dependence of fluorescence intensity of the MG/anti-MG aptamer complex at 648 nM on **S_i** concentration. This material is available free of charge via the Internet at http://pubs.acs.org.

JA051362F